

# Collinear and TMD Parton densities from fits to DIS precision data at LO and NLO

Sara Taheri Monfared<sup>1</sup>

<sup>1</sup>Deutsches Elektronen-Synchrotron DESY

REF workshop 2019-Pavia

On behalf of

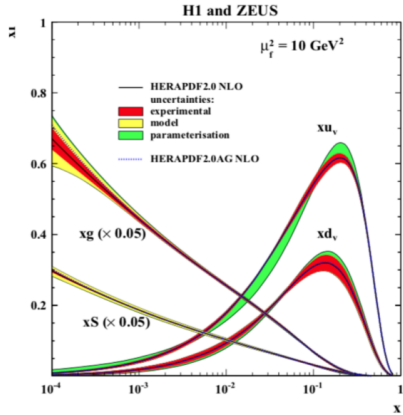
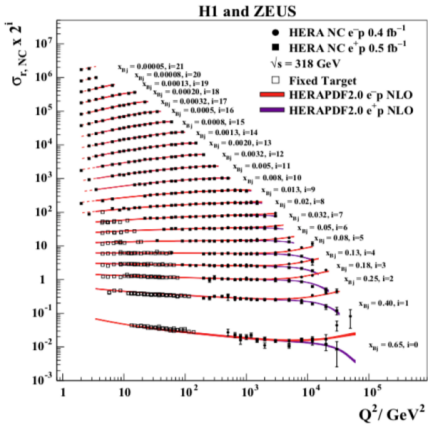
A. Bermudez Martinez, P. Connor, F. Hautmann, H. Jung, A. Lelek, V. Radescu, M. Schmitz  
and R. Žlebčík



# Outline

- 1 From inclusive to exclusive distributions
- 2 Parton Branching method
- 3 Determination of PDFs at LO and NLO
- 4 What is the gain with exclusive evolution?

# Inclusive cross section and inclusive PDFs



- **HERAPDF2.0**: available in LHAPDF for collinear calculations.

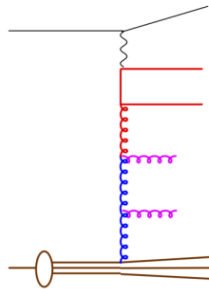
H. Abramowicz *et al.* [H1 and ZEUS Collaborations], Eur. Phys. J. C 75, no. 12, 580 (2015) [[arXiv:1506.06042 \[hep-ex\]](https://arxiv.org/abs/1506.06042)].

# From inclusive to exclusive PDFs

- standard parton density evolution is inclusive:
  - $f(x, \mu^2)$  gives probability to find parton at  $x$  and  $\mu^2$
  - no information** about the history of evolution
  - no information** about parton emissions at  $p_T$  and  $y$ 
    - is enough for inclusive calculations not for exclusive processes.
- Our physics picture and intuition is not inclusive:
  - parton evolution proceeds via real parton emissions
- Formula exclusive evolution equation for parton densities :

new approach: **Parton Branching Method**

- cover all transverse momenta from small  $k_t$  to large  $k_t$  as well as large range in  $x$  and  $\mu^2$ .



# TMDs- How to determine?

Transverse momentum effects are naturally coming from

- intrinsic  $k_t$
- **parton shower**

Determine integrated PDFs from PB solution of evolution equation:

- check consistency with standard evolution on integrated PDFs
- at LO, NLO and NNLO
- advantages of PB method  
(full freedom of choosing renormalization/evolution scale ...)

Determine TMD:

- since each branching is generated explicitly, energy-momentum conservation is fulfilled and transverse momentum distributions can be obtained.

# How to solve DGLAP evolution with PB method?

- Including the  $\Delta_s$  in to the differential form of the DGLAP eq.

$$\mu^2 \frac{\partial}{\partial \mu^2} \frac{f(x, \mu^2)}{\Delta_s(\mu^2)} = \int \frac{dz}{z} \frac{\alpha_s}{2\pi} \frac{\mathcal{P}(z)}{\Delta_s(\mu^2)} f\left(\frac{x}{z}, \mu^2\right)$$

- Integral form with a very simple physical interpretation:

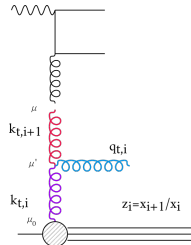
$$f(x, \mu^2) = f(x, \mu_0^2) \Delta_s(\mu^2) + \int \frac{dz}{z} \frac{d\mu'^2}{\mu'^2} \cdot \frac{\Delta_s(\mu^2)}{\Delta_s(\mu'^2)} P^R(z) f\left(\frac{x}{z}, \mu'^2\right)$$

- Solve integral equation via iteration:

$$f_0(x, \mu^2) = f(x, \mu_0^2) \Delta_s(\mu^2)$$

$$f_1(x, \mu^2) = f(x, \mu_0^2) \Delta_s(\mu^2)$$

$$+ \int_{\mu_0^2}^{\mu^2} \frac{d\mu'^2}{\mu'^2} \frac{\Delta_s(\mu^2)}{\Delta_s(\mu'^2)} \int \frac{dz}{z} P^R(z) f(x/z, \mu_0^2) \Delta_s(\mu'^2)$$



- iterating with second branching and so on to get the full solution

# Evolution equation and parton branching method

- use momentum weighted PDFs with real emission probability

$$xf_a(x, \mu^2) = \Delta_a(\mu^2) xf_a(x, \mu_0^2) + \sum_b \int_{\mu_0^2}^{\mu^2} \frac{d\mu'^2}{\mu'^2} \frac{\Delta_s(\mu^2)}{\Delta_a(\mu'^2)} \int_x^{z_M} dz P_{ab}^R(\alpha_a, z) \frac{x}{z} f_b(x/z, \mu^2)$$

- due to step by step individual branchings, all kinematics can be calculated exactly.
- $z_M$  introduced to separate real from virtual and non-resolvable branching
- reproduces DGLAP up to  $\mathcal{O}(1 - z_M)$
- make use of momentum sum rule to treat virtual corrections
- use Sudakov form factor for non-resolvable and virtual corrections

$$\Delta_a(z_M, \mu^2, \mu_0^2) = \exp \left( - \sum_b \int_{\mu_0^2}^{\mu^2} \frac{d\mu'^2}{\mu'^2} \int_0^{z_M} dz z P_{ba}^R(\alpha_s, z) \right)$$

# Determination of PDFs

# PDFs from PB method: fit to HERA data

- A kernel obtained from the MC solution of the evolution equation for any initial parton
- Kernel is folded with the non-perturbative starting distribution

$$\begin{aligned} xf_a(x, \mu^2) &= x \int dx' \int dx'' \mathcal{A}_{0,b}(x') \tilde{\mathcal{A}}_a^b(x'', \mu^2) \delta(x'x'' - x) \\ &= \int dx' \mathcal{A}_{0,b}(x') \cdot \frac{x}{x'} \tilde{\mathcal{A}}_a^b\left(\frac{x}{x'}, \mu^2\right) \end{aligned}$$

- Fit performed using xFitter frame (with collinear Coefficient functions at both **LO & NLO**)
- LO PDFs are of especial interest for MC event generators, based on LO ME + PS.
  - full coupled-evolution with all flavors
  - using full HERA I+II inclusive DIS (neutral current, charged current) data
  - $3.5 < Q^2 < 50000 \text{ GeV}^2$  &  $4.10^{-5} < x < 0.65$
- Can be easily extended to include any other measurement for fit.

A. Martinez, P. Connor, H. Jung, A. Lelek, R. Žlebčík, F. Hautmann and V. Radescu, Phys. Rev. D **99**, no. 7, 074008 (2019).

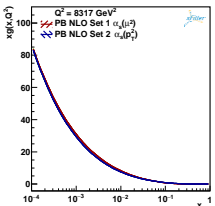
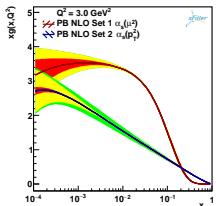
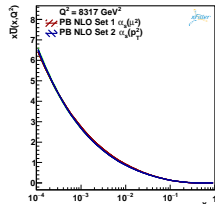
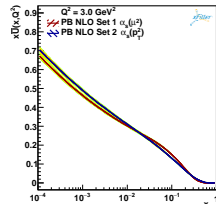
# PDFs from PB method: fit to HERA data

- Two angular ordered sets with different argument in  $\alpha_s$  (either  $\mu$  or  $q_t$ )
- $q_{cut}$  in,  $\alpha_s(\max(q_{cut}^2, |q_{t,i}^2|))$ , to avoid the non-perturbative region,  $|q_{t,i}^2| = (1 - z_i)^2 \mu_i^2$
- $\mu_0^2 = 1.9 \text{ GeV}^2$  for set1 (as in HERAPDF)
- $\mu_0^2 = 1.4 \text{ GeV}^2$  for set2 (the best  $\chi^2/\text{dof}$ )
- The experimental uncertainties defined with the Hessian method with  $\Delta\chi^2 = 1$ .
- The model dependence obtained by varying charm and bottom masses and  $\mu_0^2$ .
- The uncertainty coming from the  $q_{cut}$  in set2

	Central value	Lower value	Upper value
PB Set1 $\mu_0^2$ ( $\text{GeV}^2$ )	1.9	1.6	2.2
PB Set 2 $\mu_0^2$ ( $\text{GeV}^2$ )	1.4	1.1	1.7
PB Set 2 $q_{cut}$ ( $\text{GeV}$ )	1.0	0.9	1.1
$m_c$ ( $\text{GeV}$ )	1.47	1.41	1.53
$m_b$ ( $\text{GeV}$ )	4.5	4.25	4.75

A. Martinez, P. Connor, H. Jung, A. Lelek, R. Žlebčík, F. Hautmann and V. Radescu, Phys. Rev. D 99, no. 7, 074008 (2019).

# Standard NLO full fit with different scale in $\alpha_s$



- Set1- $\alpha_s(\mu^2) \rightarrow \chi^2/\text{dof} = 1.2$
- Set2- $\alpha_s(p_T^2) \rightarrow \chi^2/\text{dof} = 1.21$

$$xg(x) = A_g x^{B_g} (1-x)^{C_g} - A'_g x^{B'_g} (1-x)^{C'_g},$$

$$xu_v(x) = A_{u_v} x^{B_{u_v}} (1-x)^{C_{u_v}} (1 + E_{u_v} x^2),$$

$$xd_v(x) = A_{d_v} x^{B_{d_v}} (1-x)^{C_{d_v}},$$

$$x\bar{U}(x) = A_{\bar{U}} x^{B_{\bar{U}}} (1-x)^{C_{\bar{U}}} (1 + D_{\bar{U}} x),$$

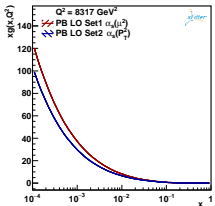
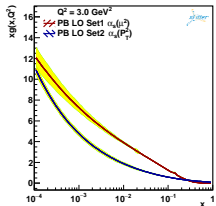
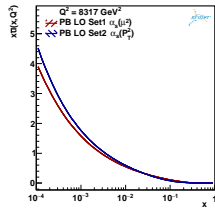
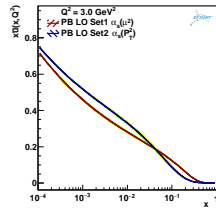
$$x\bar{D}(x) = A_{\bar{D}} x^{B_{\bar{D}}} (1-x)^{C_{\bar{D}}}.$$

- Fits are as good as HERAPDF2.0.
- Very different gluon distribution obtained at small  $Q^2$
- The differences are washed out at higher  $Q^2$

A. Martinez, P. Connor, H. Jung, A. Lelek, R. Žlebčík, F. Hautmann and V. Radescu, Phys. Rev. D 99, no. 7, 074008 (2019).

# Standard LO full fit with different scale in $\alpha_s$

NEW!



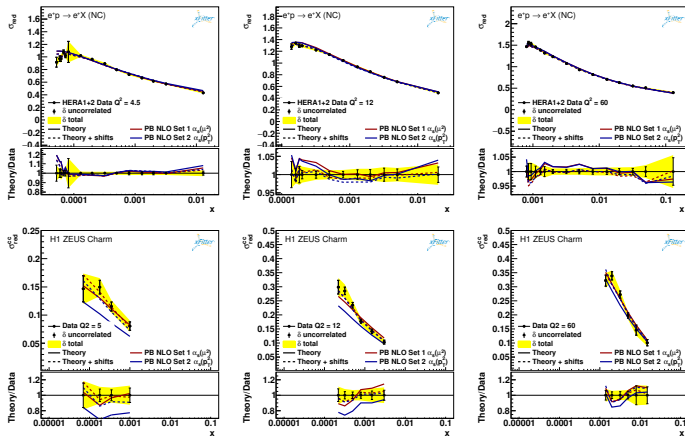
- Set1- $\alpha_s(\mu^2) \rightarrow \chi^2/dof = 1.24$
- Set2- $\alpha_s(p_T^2) \rightarrow \chi^2/dof = 1.37$

$$\begin{aligned}
 xg(x) &= A_g x^{B_g} (1-x)^{C_g}, \\
 xu_v(x) &= A_{uv} x^{B_{uv}} (1-x)^{C_{uv}} (1+E_{uv}x^2), \\
 xd_v(x) &= A_{dv} x^{B_{dv}} (1-x)^{C_{dv}}, \\
 x\bar{U}(x) &= A_{\bar{U}} x^{B_{\bar{U}}} (1-x)^{C_{\bar{U}}} (1+D_{\bar{U}}x), \\
 x\bar{D}(x) &= A_{\bar{D}} x^{B_{\bar{D}}} (1-x)^{C_{\bar{D}}}.
 \end{aligned}$$

- Very different gluon distribution obtained at small and large  $Q^2$
- The differences exist at higher  $Q^2$

# Fit to DIS x-section at NLO: $F_2$ and $F_2^c$

How well can we describe inclusive DIS cross section and inclusive charm production with the two sets at NLO?

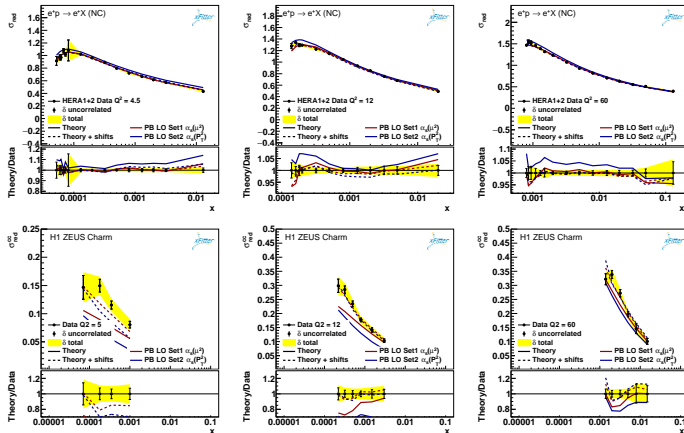


A. Martinez, P. Connor, H. Jung, A. Lelek, R. Žlebčík, F. Hautmann and V. Radescu, Phys. Rev. D 99, no. 7, 074008 (2019).

# Fit to DIS x-section at LO: $F_2$ and $F_2^c$

How well can we describe inclusive DIS cross section and inclusive charm production with the two sets at LO?

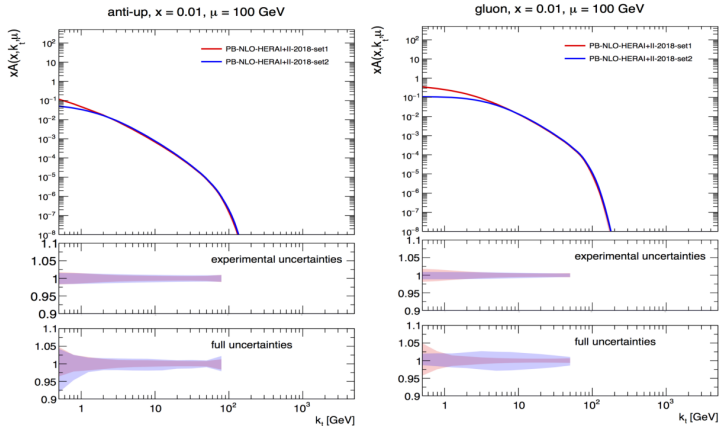
NEW!



On the inclusive level, DIS cross section and charm production are well described.

## **What is the gain with exclusive evolution?**

# TMD distributions from fit to HERA data

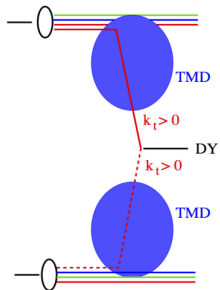


- Different shape and dependence of the uncertainty as a function of  $k_t$ .
- Model dependence larger than experimental uncertainties.
- Difference essentially in low  $k_t$  region.
- Introducing  $p_T$  instead of  $\mu$  suppresses further soft gluons at low  $k_t$ .

# Application to DY $q_T$ - spectrum

- fixed-order perturbative calculations cannot describe transverse momentum spectrum of Z bosons in DY at small  $q_T$ .

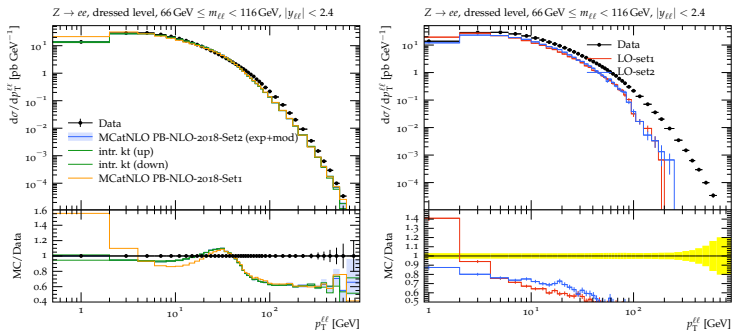
- Use LO ME  $q\bar{q} \rightarrow z_0$
- add  $k_t$  for each parton as function of  $x$  and  $\mu$  according to TMD
- keep final state mass fixed:
  - $x_1$  and  $x_2$  are different after adding  $k_t$



# Application to DY $q_T$ - spectrum

Transverse momentum spectrum of Z-bosons obtained from two **NLO** and **LO** TMDs, compared with ATLAS measurements. :

- TMD with angular ordering including  $\alpha_s(\mu^2)$
- TMD with angular ordering including  $\alpha_s(p_T^2)$  → Qun's talk for NLO DY spectrum



ATLAS Collaboration Eur. Phys. J. C76 (2016),291, arXiv:1512.02192 [hep-ph].

A. Martinez, P. Connor, H. Jung, A. Lelek, R. Žlebčík, F. Hautmann and V. Radescu, Phys. Rev. D 99, no. 7, 074008 (2019).

A. Bermudez Martinez *et al.*, Phys. Rev. D 100, no. 7, 074027 (2019).

# Conclusion

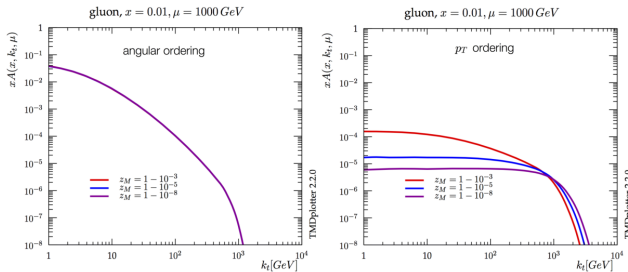
- PB method to solve DGLAP equation at LO, NLO, NNLO.
  - consistent for collinear (integrated) PDFs shown
  - advantages of PB method (angular ordering)
- method directly applicable to determine  $k_t$  distribution (as would be done in PS)
  - TMD distributions for all flavors determined at LO & NLO
  - TMD evolution implemented in xFitter -fits to processes at the moment
- Application to pp processes:
  - DY  $q_T$ -spectrum without new parameters

# Thank you for your attention

# Backup

# Transverse Momentum Dependence

- Parton Branching evolutions generates every single branching. Kinematics can be calculated at every step.
- Give physics interpretation of evolution scale:
  - $p_T$ -ordering :  $\mu = q_T$
  - angular ordering :  $\mu = q_T / (1 - z)$



- $p_T$ -ordering shows significant dependence on  $Z_M$ : Unstable results because of soft gluon contribution.
- angular ordering is independent of  $Z_M$ : stable results since soft gluons are suppressed.

# intrinsic $k_{t,0}$ distribution

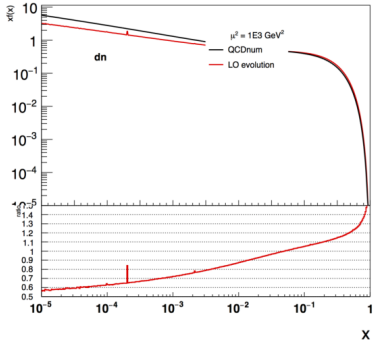
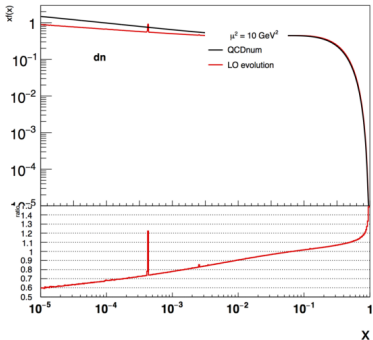
$$\begin{aligned} xf_a(x, \mu^2) &= x \int dx' \int dx'' \mathcal{A}_{0,b}(x') \tilde{\mathcal{A}}_a^b(x'', \mu^2) \delta(x'x'' - x) \\ &= \int dx' \mathcal{A}_{0,b}(x') \cdot \frac{x}{x'} \tilde{\mathcal{A}}_a^b\left(\frac{x}{x'}, \mu^2\right) \end{aligned}$$

$$\mathcal{A}_{0,b}(x, k_{t,0}^2) = f_{0,b}(x) \cdot \exp(-|k_{t,0}^2|/\sigma^2)$$

where the intrinsic  $k_{t,0}$  distribution is given by a Gauss distribution with  $\sigma^2 = q_0^2/2$  for all flavors and all  $x$  with a constant value  $q_0 = 0.5$  GeV.

# Effect of LO vrs NLO evolution

Using the same starting distribution, but LO or NLO splitting functions

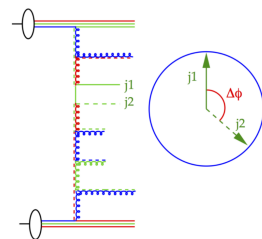
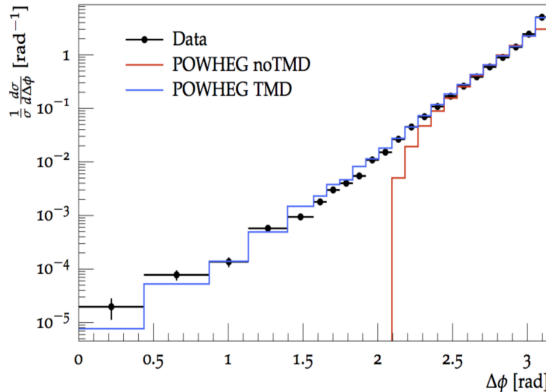


- effect of NLO evolution ( $\alpha_s$  and  $P_{ij}$ ) is very large:  $\sim 50\%$  for quarks

NB: spikes in plots come from fluctuations in MC solution.

# Why TMDs?

Di-jet azimuthal decorrelation,  $300 < p_T^{\text{leading}} < 400 \text{ GeV}$



- NLO-dijet with collinear POWHEG cannot describe small  $\Delta\phi$
- NLO-dijet with TMD POWHEG describes spectrum at small and large  $\Delta\phi$
- Region of higher order emissions described by TMDs. This approach improves the description of jet production.